Table S1. Metadata human postmortem brain tissue

Sample nr	PM delay	AAO	AAD	Duration	Gender	Clinical Diag	Path Diag	Cleanedpathdiag	Brain Weight	APOE	Braak Tau	Thal Phase	CERAD	ABC	CAA
1	34:00:00	54	63	9	M	Picks/FTD (bvFTD)	AD	AD	1150	44	6	5	3	A3B3C3	2
2	90:05:00	64	77	13	M	AD (Amnestic)	AD	AD	1264	44	6	5	3	A3B3C3	3
3	60:25:00	59	76	17	F	AD	AD	AD	1191	44	6	5	3	A3B3C3	2
4	70:00:00	55	68	13	M	DLB	AD	AD	1522	33	6	5	3	A3B3C3	1
5	76:40:00	49	62	13	F	AD (Amnestic)	AD	AD	996	33	6	5	3	A3B3C3	0
6	84:45:00	58	69	11	M	PPA / AD	AD	AD	1600	33	6	5	3	A3B3C3	3
7	61:19:00	63	79	16	M	AD	AD	AD	1423	33	6	5	3	A3B3C3	3
8	78:15:00	69	81	12	M	AD	AD	AD	1116	33	6	5	3	A3B3C3	2
9	31:42:00	48	63	15	M	AD	AD	AD	1042	33	6	5	3	A3B3C3	3
10	34:25:00	54	65	11	M	AD	AD	AD	1089	44	6	5	3	A3B3C3	3
11	17:10:00	55	67	12	F	PPA	AD	AD	1009	33	6	5	3	A3B3C3	3
12	14:50:00	62	72	10	M	PD	AD	AD	1180	44	6	5	3	A3B3C3	2
13	66:00:00	51	60	9	F	CBD	AD	AD	1090	33	6	5	3	A3B3C3	3
14	33:26:00	63	74	11	M	AD	AD	AD	1022	44	6	5	3	A3B3C3	3
15	44:05:00	68	84	16	F	VD	AD	AD	1127	44	6	5	3	A3B3C3	3
16	45:35:00	52	71	19	M	AD	AD	AD	1097	33	6	5	3	A3B3C3	3
17	52:30:00	53	68	15	F	Picks	AD	AD	1103	44	6	5	3	A3B3C3	1
18	40:10:00	49	69	20	F	AD	AD	AD	986	44	6	5	2	A3B3C2	3
19	92:47:00	50	66	16	F	Picks (PPA) (Amnestic)	AD	AD	906	33	6	5	3	A3B3C3	2
20	30:25:00	59	79	20	F	AD	AD	AD	961	33	6	5	3	A3B3C3	3
21	80:00:00		64		M	Control	Control	Control	1695	33	0	1	0	A1B0C0	0
22	47:00:00		73		M	Control	Control	Control	1291	33	4	1	0	A0B2C0	0
23	171:00:00		69		M	Control	Control/path aging	Control	1435	33	1	3	1	A2B1C1	0
24	26:46:00		70		F	Dystonia?	Control	Control	1200	23	1	0	0	A0B1C0	0
25	79:00:00		76		M	Control	Control	Control	1366	34	2	1	0	A1B1C0	0
26	24:00:00		73		F	Control	Path Ageing	Control	1214	34	2	2	2	A1B1C2	1
27	76:10:00		71		F	Control	Control	Control	1214	33	3	2	1	A1B1C0	2
28	47:05:00		89		M	Control	Control	Control	1356	33	2	3	1	A2B1C1	1
29	29:30:00		78		F	Control	Control age related changes	Control	1225	22	2	0	0	A0B2C0	0
30	88:50:00		79		F	Control	Control	Control	1288	33	1	2	1	A2B1C1	0
31	45:05:00		68		F	Control	Control	Control	1330	23	0	0	0	A0B0C0	0
32	54:20:00		73		M	Control	Control	Control	1498	24	3	4	2	A3B2C2	3
33	3:30:00		79		M	Control	Control	Control	1355	33	2	0	0	A0B1C0	0

Supplementary figures

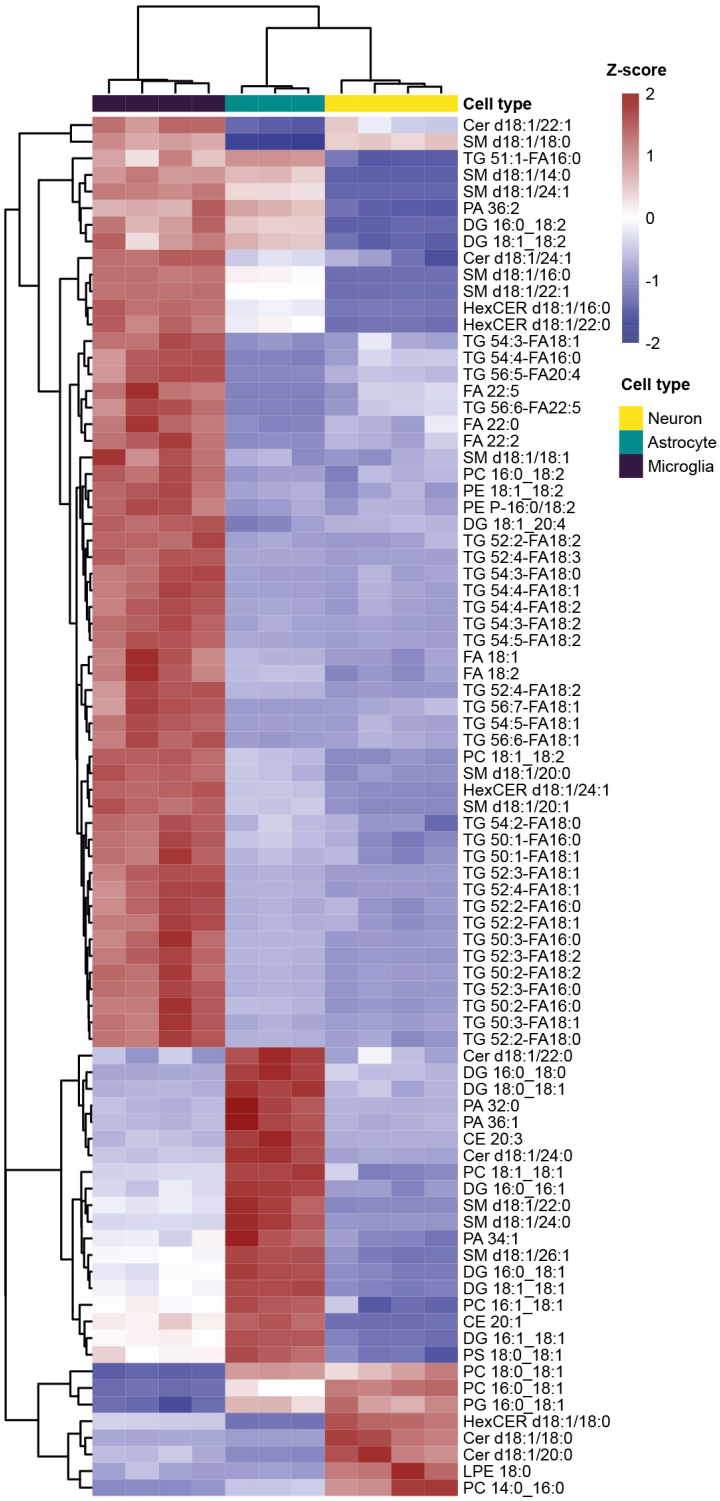

Supplementary Figure 1. Lipotypes (most differentiating species) of human iPSC-derived neurons, astrocytes and microglia A) Heatmap of most differentiating lipid species different between iPSC-derived neurons, astrocytes and microglia. alpha = 0.8.

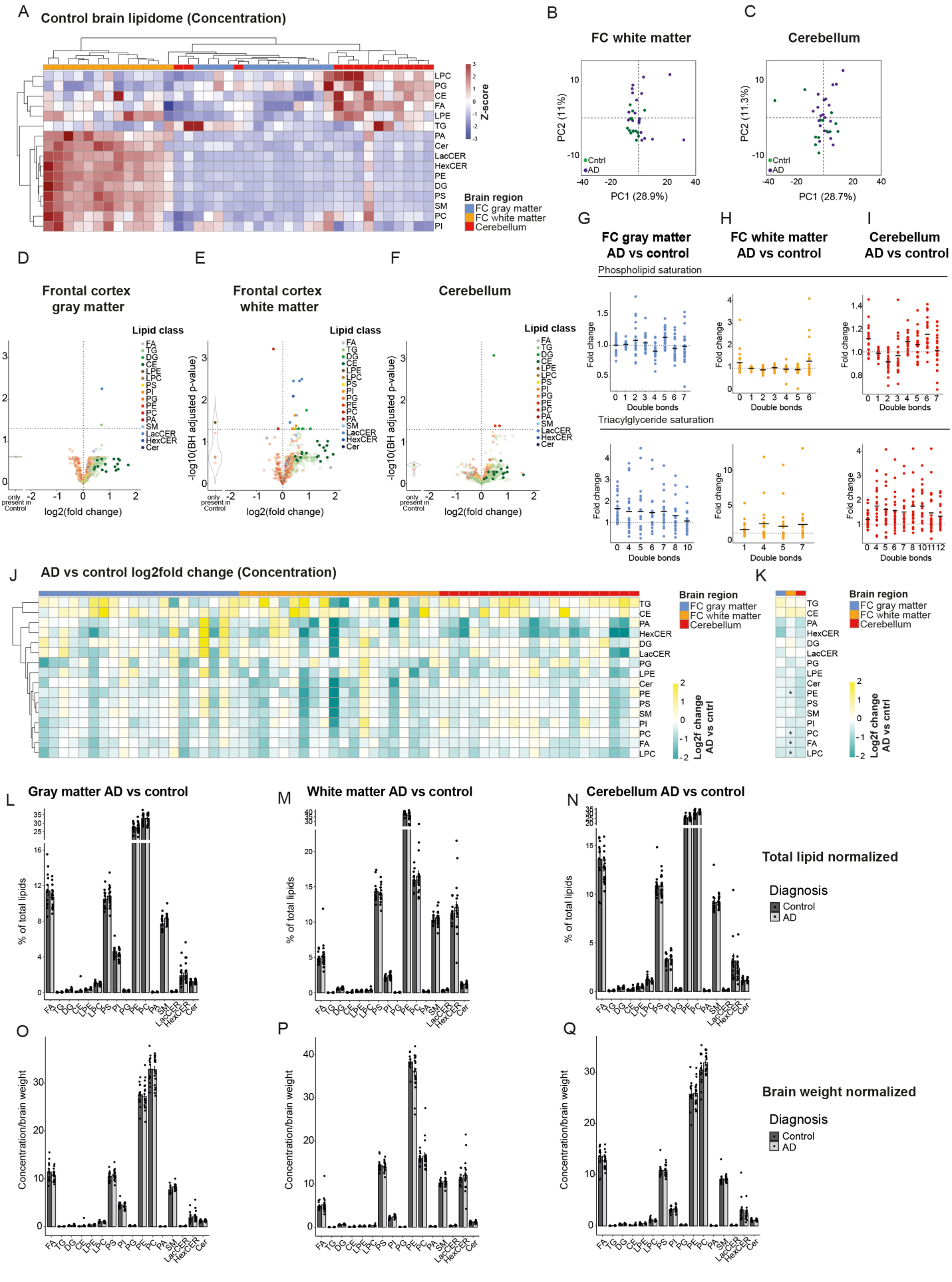

Supplementary Figure 2. Extended analysis of human (AD) brain lipidomics A) Heatmap with Z-scored lipid class concentrations (nmol/mg brain material) from indicated brain regions (control subjects only). B-C) PCA plot of unbiased lipidomic analysis of AD (purple) and control (green) brain tissue samples from (FC) white matter (B) and Cerebellum (C). D-F) Volcano plots of individual lipid species in AD vs control brain tissue for FC gray matter (D), FC white matter (E) and Cerebellum (F) as a % of total lipidome. CE species are highlighted. G-I) Fold change of phospholipid and TG species with indicated number of double bonds in AD vs control samples from FC gray matter (G), FC white matter (H) and Cerebellum (I) from % of total lipids. J) Heatmap depicting changes in lipid classes (concentrations) for individual AD samples compared to the average of control samples. Log2fold change plotted independent for each donor and each brain area. K) Average log2fold change in AD subject group compared to control samples per lipid class and brain area. Data from (J). L-N) Bar graphs present individual lipid class changes in FC gray matter (L), FC white matter (M) and Cerebellum (N) in AD versus control samples (group level) as % of total lipids. O-Q) Bar graphs present individual lipid class levels in FC gray matter (O), FC white matter (P) and Cerebellum (Q) in AD and control samples (group levels) as concentrations.

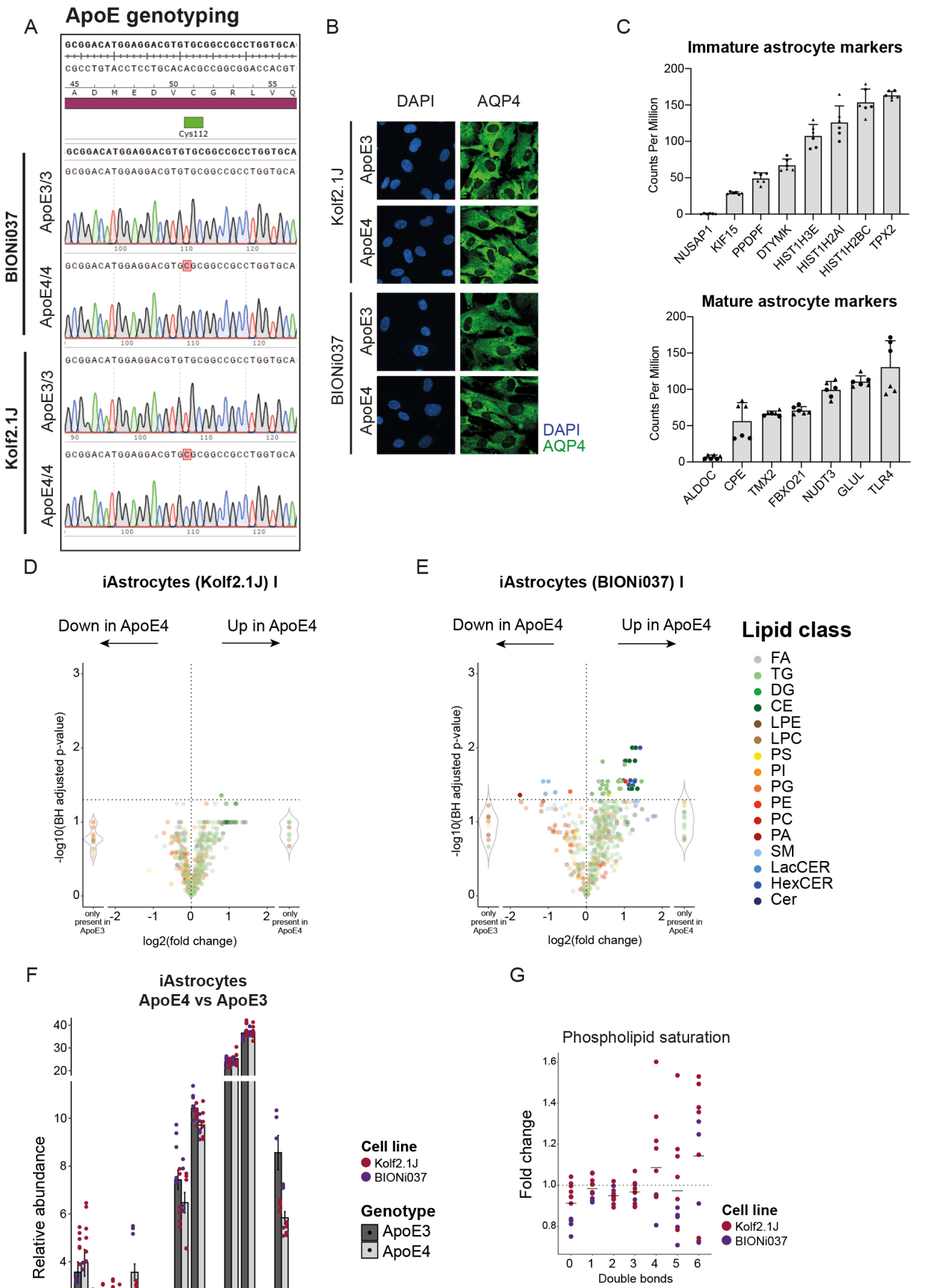

Supplementary Figure 3. Extended lipidomic analysis of human isogenic APOE3/3 and APOE4/4 iPSC-derived astrocytes A) Representative sequencing result for confirming cell identity and expected ApoE genotype B) Image of differentiated iAstrocytes, from both BIONi037 and Kolf2.1J lines. Scale bar = 25mm C) Gene expression levels (as determined by RNAseq) of indicated mature and immature astrocyte markers in our iPSC-derived astrocytes. n=6 wells BIONi037 (n=3 ApoE3 n=3 ApoE4) D-E) Volcano plots of lipid species in Kolf2.1J (D) or BIONi037 (E) ApoE4 vs ApoE3 iAstrocytes from a second independent lipidomics experiment. n=3 wells for Kolf2.1J, n=2 for BIONI037 (one BIONi037 ApoE4 sample was removed as outlier). F) Bar graphs of lipid classes in ApoE3 and ApoE4 iAstrocytes from BIONi037 and Kolf2.1J background (% of total). n=6 samples Kolf2.1J n=5 BIONI037 G) Fold change of phospholipid species with indicated number of double bonds in ApoE4 vs ApoE3 iAstrocytes.

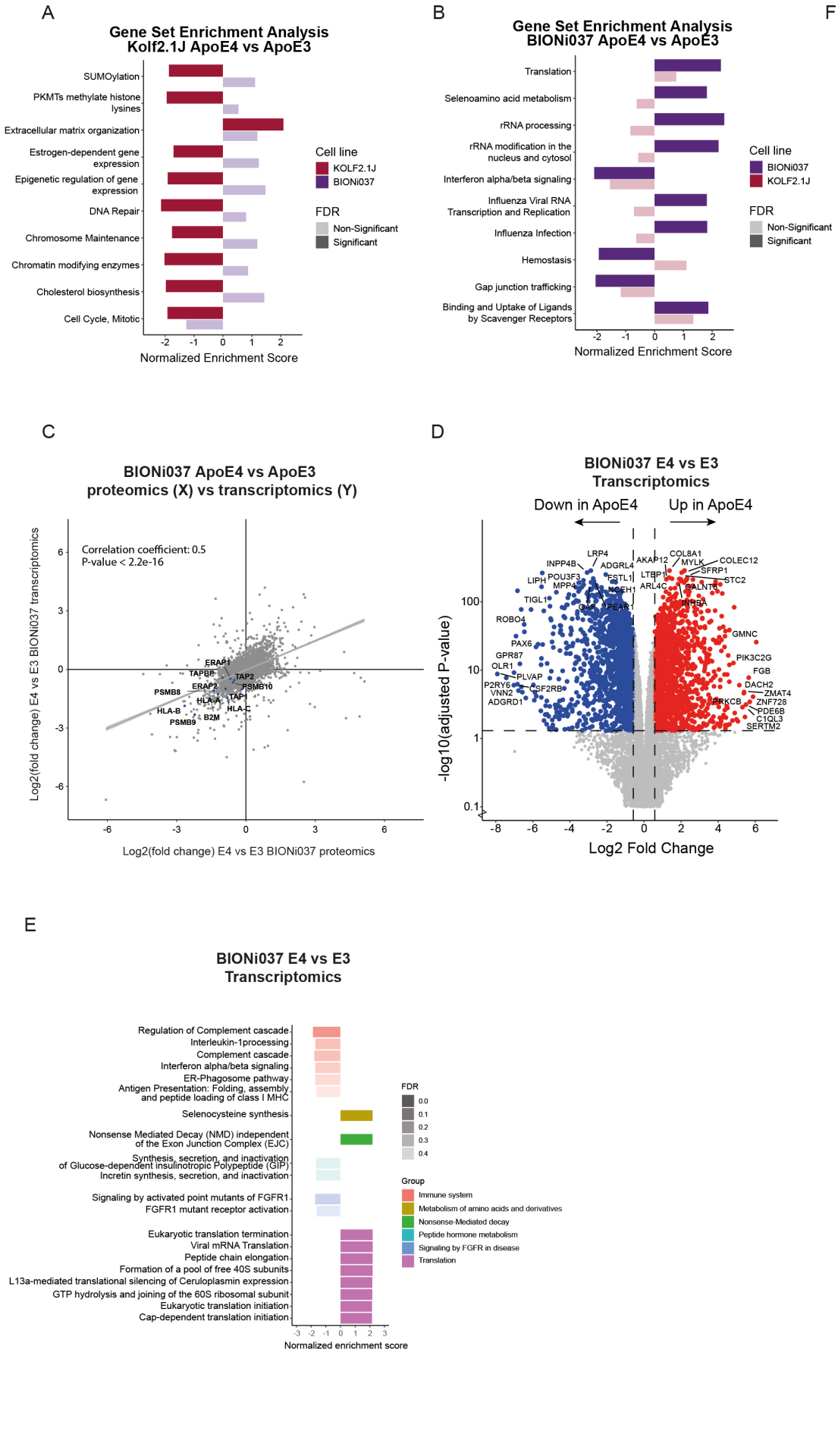

Supplementary Figure 4. Extended proteomic and transcriptomic analysis of human isogenic APOE3/3 and APOE4/4 iPSC-derived astrocytes A-B) Gene-set enrichment analysis was performed on proteomics data from ApoE4 versus ApoE3 iAstrocytes for the Kolf2.1J and the BIONi037 lines. Plotted are the enrichment scores (for both lines) for the reactome pathways significantly enriched in Kolf2.1J (A) and pathways significantly enriched in BIONI037 (B). C) Scatterplot of changes in protein levels (as measured by proteomics) versus changes in matching RNA expression (transcriptomics) in BIONi037 ApoE4 vs ApoE3 iAstrocytes. MHC-I and immunoproteasome pathway genes are indicated. D-F) Heatmaps showing changes of indicated genes in ApoE4 vs ApoE3 iAstrocytes from our study and previous studies (as indicated) within consistently altered pathways as identified by transcriptomics in Figure 4K. G) Transcriptomics data from ApoE4 vs ApoE3 BIONi037 iAstrocytes. Log2fold change of differentially expressed genes (DEGs) in ApoE4 vs ApoE3 astrocytes. Top ten genes with highest log2fold change and top ten genes with most significant P-value are labeled. n=3 wells per genotype. H) Top 10 reactome pathways upregulated or downregulated (with lowest FDR) in ApoE4 vs ApoE3 by gene-set enrichment analysis of transcriptomics data.

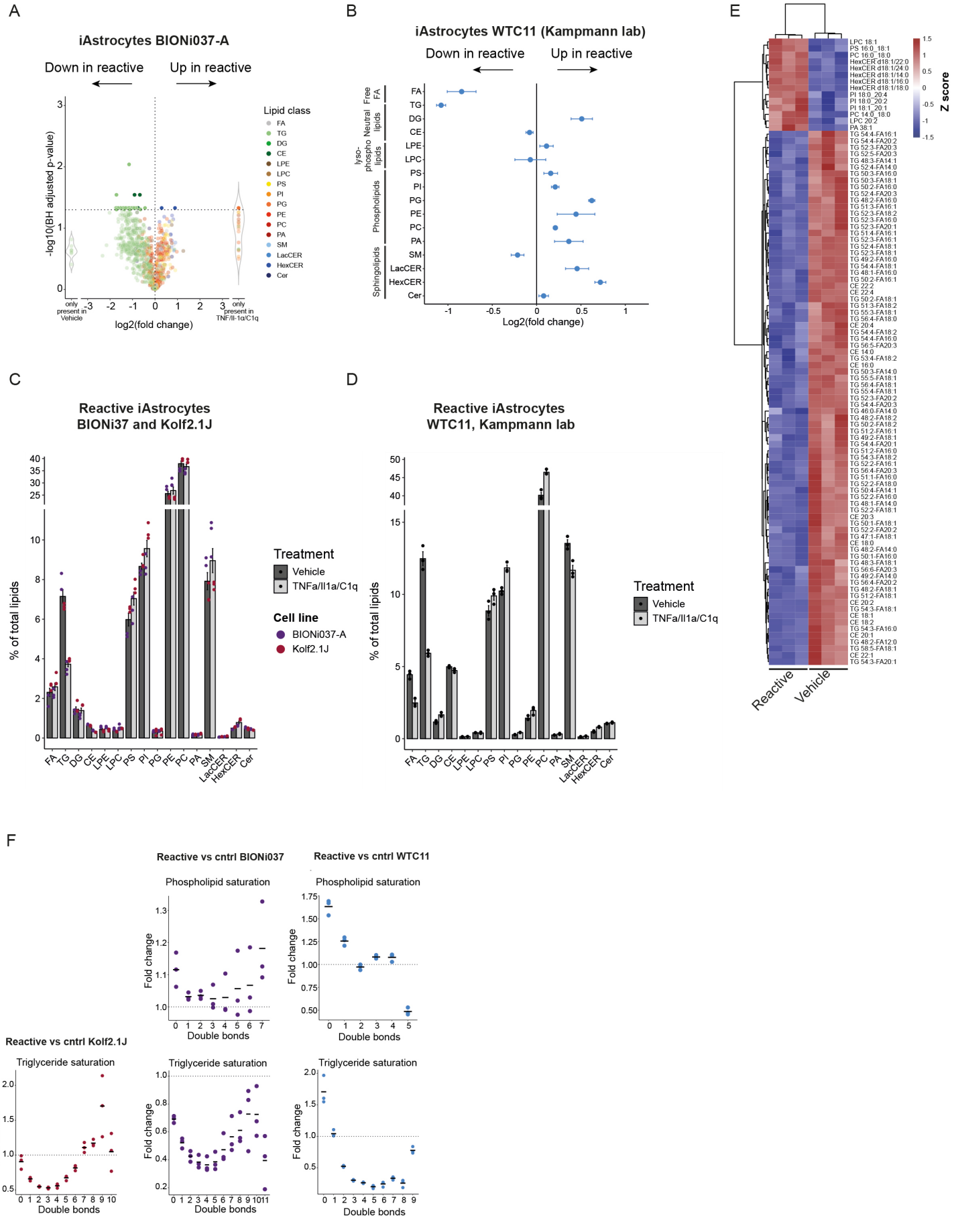

Supplementary Figure 5. Extended lipidomics analysis of reactive human iPSC-derived astrocytes A) Log2fold change of altered individual lipid species in reactive vs control iAstrocytes (BIONi037 ApoE3). n=3 wells reactive n=2 wells control. B) Summary data of changes in all detected lipid classes in reactive vs control iAstrocytes from the Kampmann lab (WTC11 iPSC line, ApoE3/3 cultured in 2% FBS). n=3 wells per condition. C-D) Bar graphs present changes in lipid classes in reactive vs control from Kolf2.1J and BIONi037 (C) or WTC11 (Kampmann lab) (D) iAstrocytes. Shown is % of total lipid, n=3 samples per line. E) Most differentiating lipid species in reactive vs control iAstrocytes (Kolf2.1J ApoE3) a=0.8. F) PL and TG saturation (number of double bonds) in Kolf2.1J, BIONi037 and WTC11 iAstrocytes.

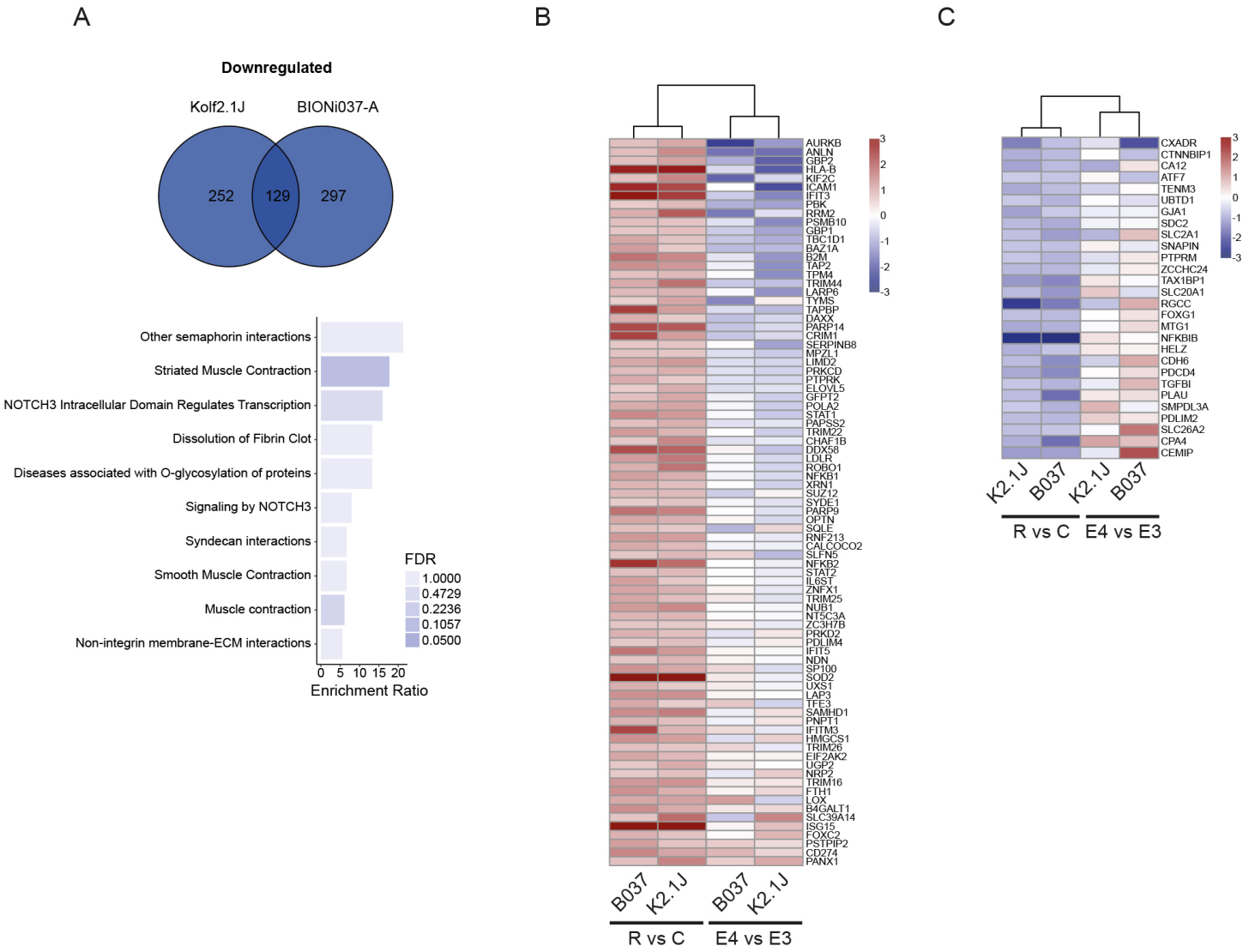

Supplementary Figure 6. Extended proteomic analysis of reactive human iPSC-derived astrocytes
A) Venn diagram depicting the number of proteins that were significantly downregulated >1.25 fold (>0.3 log2fold) in reactive Kolf2.1J, BIONi037 and both iAstrocytes. Top 10 (non-significant) enriched reactome pathways detected by overrepresentation analysis are plotted. B) Heatmap shows the log2fold change of all proteins significantly upregulated >1.5 fold in both Kolf2.1J and BIONi037 reactive astrocytes. Next are the log2fold change values of these proteins in ApoE4 vs ApoE3 iAstrocytes. C) Heatmap shows the log2fold change of all proteins significantly downregulated >1.5 fold in Kolf2.1J and BIONi037 reactive astrocytes and the log2fold change values of these proteins in ApoE4 vs ApoE3 iAstrocytes.

A

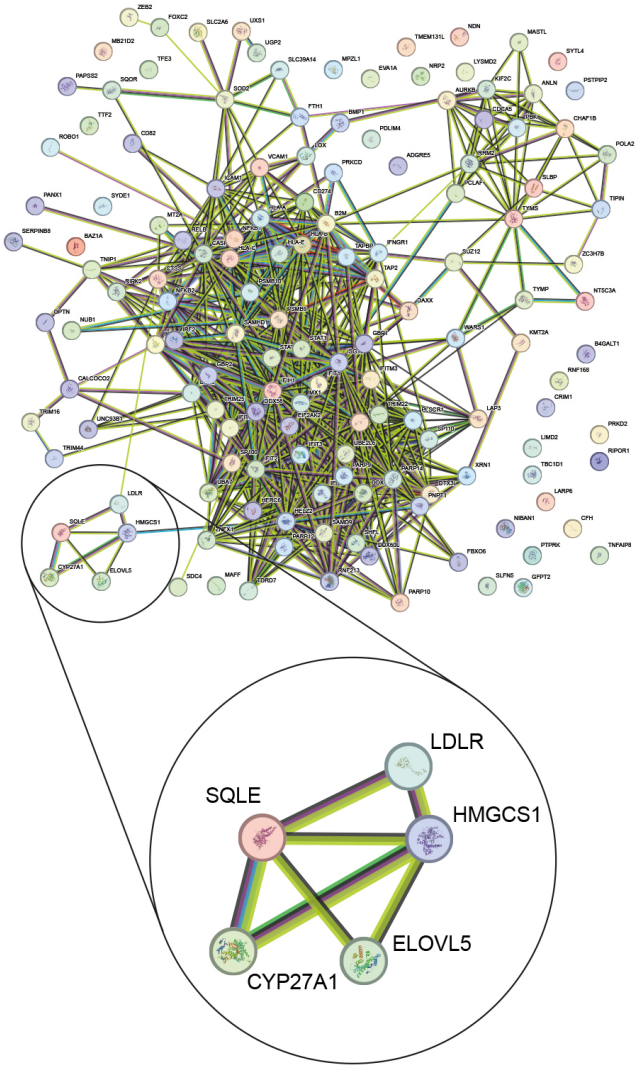

B

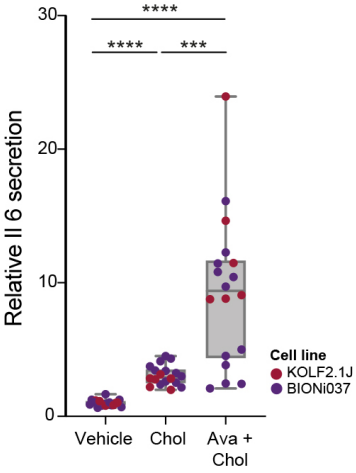

C

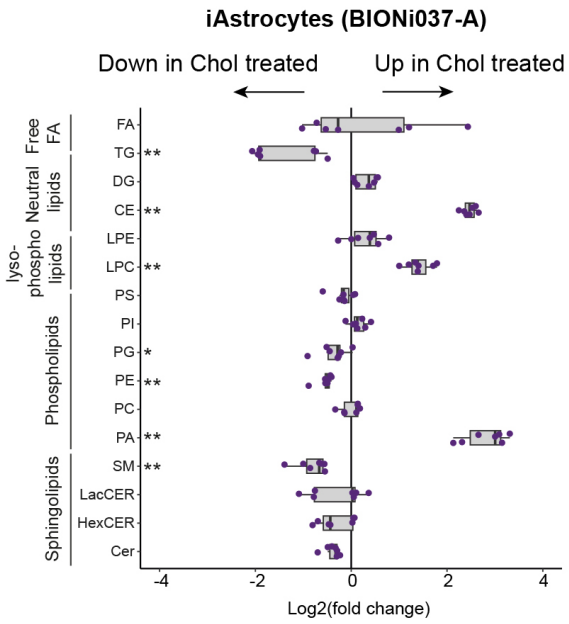

D

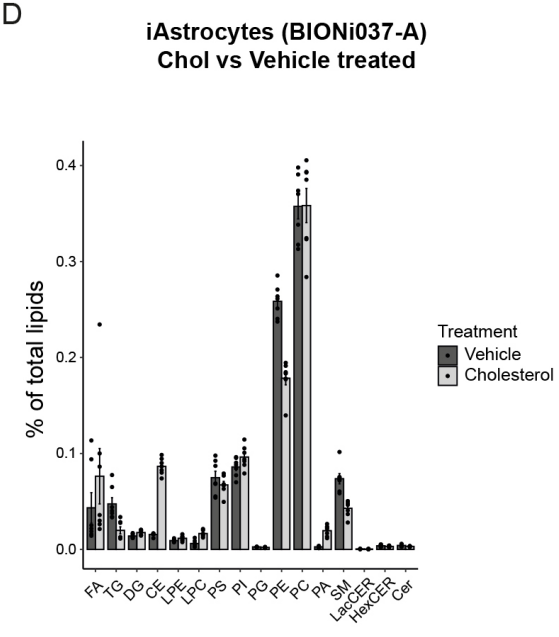

Supplementary Figure 7. Cholesterol regulates astrocyte activation extended data A) StringDB analysis of all proteins significantly upregulated >1.5 fold in Kolf2.1J and BIONi037 reactive astrocytes (dataset from figure 5). Zoom in shows cluster of genes related to cholesterol metabolism. B) Normalized Il-6 secretion in iAstrocytes (ApoE3), pre-treated with vehicle or avasimibe (0.5mM) for one hour and then treated for 24 hours with vehicle, cholesterol or cholesterol + avasimibe. n=6 (K2.1J) and n=12 (B037) from 4 independent experiments. ***P<0.001 Welch ANOVA with Dunnett's multiple testing correction C) Summary data of changes in all detected lipid classes in cholesterol vs vehicle treated iAstrocytes (BIONi037-A). n=6 wells from 3 independent experiments. Mann-Whitney U test with Benjamini-Hochberg correction *=P<0.05. D) Bar graphs of lipid classes in cholesterol vs vehicle treated iAstrocytes from BIONi037-A background (% of total). n=6 wells from 3 independent experiments.

Sample type	Experiment	Contributing lab
iPSC-derived neurons	1. Human iPSC-derived neurons. Multiple inductions from 3 C9orf72 lines and 3 isogenic Control lines (from Giblin *et al*.)	Isaacs lab
	2. Human iPSC-derived neurons. Multiple inductions from 3 C9orf72 lines treated with C9orf72-knockdown antisense oligonucleotides (from Giblin *et al*.)	Isaacs lab
	3. Human iPSC-derived neurons. Multiple inductions from 2 control lines transduced with C9orf72 repeat lentiviruses (from Giblin *et al*.)	Isaacs lab
	4. alpha-synuclein E46K neurons	Van der Kant lab
	5. TMEM106B SS185 vs TT185 vs Null iNeurons	Ward lab
iPSC-derived astrocytes	1. Control vs reactive (IL1α_TNFα_C1q) iAstrocytes in three cell lines: WTC11 Rose, BIONi037-A & KOLF2.1J (from Feringa and Koppes-den Hertog *et al*.)	Kampmann lab & Van der Kant lab
	2. Multiple repeats of ApoE4 vs ApoE3 isogenic iAstrocytes with FBS in two cell lines: BIONi037-A & KOLF2.1J	Van der Kant lab
	3. Multiple repeats of ApoE4 vs ApoE3 isogenic iAstrocytes no FBS in two cell lines: BIONi037-A & KOLF2.1J (from Feringa and Koppes-den Hertog *et al*.)	Van der Kant lab
	4. Multiple repeats of ApoE3 iAstrocytes cultured with FBS versus no FBS in two cell lines: BIONi037-A & KOLF2.1J	Van der Kant lab
iPSC-derived neurons, microglia and astrocytes	1. IPSC-derived neurons, microglia and astrocytes (from Feringa and Koppes-den Hertog *et al*.)	Van der Kant lab Kronenberg-Versteeg lab
Human brain	1. Human cerebellum AD vs control (from Feringa and Koppes-den Hertog *et al*.)	Lashley lab Van der Kant lab
	2. Human prefrontal cortex gray matter AD vs control (from Feringa and Koppes-den Hertog *et al*.)	Lashley lab Van der Kant lab
	3. Human prefrontal cortex white matter AD vs control (from Feringa and Koppes-den Hertog *et al*.)	Lashley lab Van der Kant lab
	4. Human prefrontal cortex gray matter, white matter and cerebellum all control (from Feringa and Koppes-den Hertog *et al.)*	Lashley lab Van der Kant lab
	5. Human prefrontal cortex gray matter FTLD vs control (from Giblin *et al.*)	Lashley lab Isaacs lab
	6. Human cerebellum FTLD vs control (from Giblin *et al.*)	Lashley lab Isaacs lab
Mouse brain	1. Mouse cortex ApoE4 vs ApoE3 target replacement mice 6 months old	Van der Kant lab
	2. Mouse cortex ApoE4 vs ApoE3 target replacement mice 3 months old	Van der Kant lab

Supplementary Table 1. The Neurolipid Atlas: an open access data commons for brain lipid data
Description of datasets currently available on the Neurolipid Atlas.